

Minimization of temperature cross-sensitivity of EFPI pressure sensor for oil and gas exploration and production applications in well bores

Han-Sun Choi*, Andy Cantrelle, Clark Bergeron, Paul Tubel
Tubel Technologies, Inc. 4800 Research Forest, The Woodlands, TX77381

ABSTRACT

Extrinsic Fabry-Perot Interferometer, EFPI, is a versatile device for many fiber optic sensing applications including one in harsh environments such as oil and gas wells. Due to its unique structure, the EFPI could be designed to have an extremely small temperature cross-sensitivity (TCS), by matching the coefficients of thermal expansion (CTE's) of the outer gage capillary tube and the inner fibers. Even though it is relatively easy to get a matching condition at the atmospheric pressure, it is not a good design because the CTE of the capillary tubing is expected to change under high pressure conditions.

In this paper, the method and the experimental results for the study to minimize the temperature cross-sensitivity (TCS) of the EFPI pressure sensor are presented. Test results have confirmed that the CTE of the capillary tube slightly increases under high pressure, changing the original TCS at the atmospheric pressure. By manipulating the design of the sensor to have a higher negative slope of TCS for the air-gap (dG/dT) at the atmospheric pressure, the zero TCS point can be deliberately shifted to any point of interest within the pressure range.

Keywords: Fiber Optic Pressure Sensor, EFPI, Temperature Cross-Sensitivity, Minimization of Temperature Effect

1. INTRODUCTION

As is well known, major advantages of the fiber optic sensor are immunity to electromagnetic interference, small size and light weight, resistance to harsh environment, remote operation, and avoidance of electric sparks etc. [1]. Due to these inherent advantages, a large variety of fiber optic sensor systems have been developed for various applications during the last two decades [2]. Oil and gas well bore application would be a promising field for fiber optic sensor systems because the demand for the real-time monitoring of reservoir conditions is increasing to improve production efficiency and to enhance the total recovery. The use of conventional sensors has been quite limited due to their harsh environment of high temperature and pressure with various chemicals in the crude oil.

The temperature cross-sensitivity is one of the most important performance parameters for a static pressure sensing. In the case of fiber optic pressure sensors employing Fiber Bragg Gratings (FBG's), significant temperature sensitivity is unavoidable due to the refractive index changes within the fiber core in response to the temperature variations [3]. For this type of sensor, a temperature sensor should always be collocated with the pressure sensing element, and a proper compensation should be made. The additional hardware will increase the sensor cost as well as reduce the measurement accuracy. It was reported that the temperature sensitivity can be reduced dramatically by use of polarization maintaining (PM) fibers as pressure sensing element [4, 5]. However these sensors need return path of fiber and are inconvenient to be used in down-hole applications not to mention the overall performance of using the PM fibers as sensing elements. Extrinsic Fabry-Perot Interferometer, EFPI, is a versatile device for many fiber optic sensing applications [6, 7]. Due to its unique structure of the air-gap between the two Fresnel reflectors formed by two fiber-cleaved ends in a capillary tube, it could be designed to have a very negligible temperature cross-sensitivity (TCS) for down-hole pressure sensing applications.

Our goal is the implementation of low cost and high performance commercialization of fiber optic pressure sensor which can be widely used in the oil and gas field. In this paper, part of the effort for the goal is introduced. Fig 1 and Fig 2 show the sensor fabrication setup and the surface system respectively. A CO₂ laser is used for the glass parts welding. The surface system comprises an LED source, a fiber coupler, a spectrometer and a digital signal processor for the demodulation of the pressure signal. All the components are low cost version. Tubel Technologies Inc. (TTI) has developed a novel software algorithm to accurately demodulate the air-gap of the EFPI without the fringe jumping problem. All the experiments have been performed successfully using the new demodulation algorithm.

*han-sun.choi@tubeltechnologies.com; phone 1 281 367-1348 Ext. 3017; fax 1 281 363-7935; tubeltechnologies.com

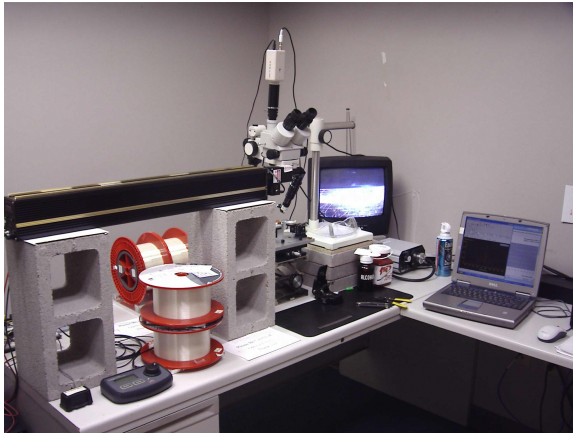


Fig. 1. Sensor fabrication setup with CO2 laser



Fig. 2. Surface system including demodulator

2. EFPI pressure sensor and its temperature cross-sensitivity

The earlier generation of the EFPI sensor used an epoxy to bond the fibers and capillary tube. Due to the temperature limitations and the high creep amount of the epoxy material, CO2 laser has been used for the bonding of the glass parts since a few years ago. Fig. 3 shows the structure of an EFPI pressure sensor. The air-gap (G) response due to the pressure is typically very linear and predictable. It is a function of the capillary tube material characteristics and the tube dimensions such as inner and outer diameter, gage length (L_0 in the Fig 3). The air-gap change, ΔG , due to an applied pressure P can be expressed as [6]:

$$\Delta G = \frac{L_0 \cdot (P - P_0) \cdot r_o^2}{E \cdot (r_o^2 - r_i^2)} \cdot (1 - 2\mu) \quad (1)$$

Where L_0 is the sensor gage length between the two bonding points, P_0 is the pressure inside the tube which is approximately the atmospheric pressure, E is the Young's Modulus of the glass material used for the capillary tube, r_o and r_i are outer and inner radius of the glass tube, and μ is the Poisson's ratio of the glass.

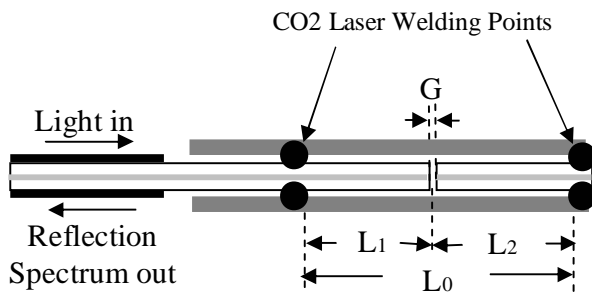


Fig. 3. Structure of EFPI pressure sensor

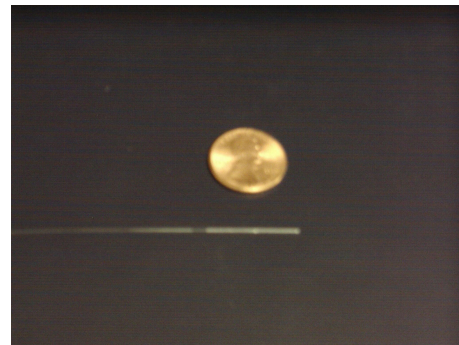


Fig. 4. An EFPI pressure sensor before packaging

The air-gap G is typically very small in comparison to the gage length L_0 . Given this condition, as long as the thermal expansion coefficients (CTE) for the glass tube and the fibers inside are matched, the temperature cross-sensitivities (TCS) for this type of sensors can be negligibly small. Optical fiber uses fused silica for its base material. The CTE for an optical fiber is quite close to the fused silica which is $\sim 0.5 \times 10^{-7} / ^\circ\text{C}$. However depending on the doping material

and the doping level of its core and the size of the core, the CTE's slightly vary for different fibers. TCS or $\Delta G / \Delta T$ can be described as [6]:

$$\frac{\Delta G}{\Delta T} = \alpha_0 \cdot L_0 - (\alpha_1 \cdot L_1 + \alpha_2 \cdot L_2) \quad (2)$$

Where $\alpha_0, \alpha_1, \alpha_2$ are the thermal expansion coefficients (CTE) of the capillary tube, the input fiber, and the reflector fiber respectively, and L_1, L_2 are the lengths of the input fiber and the reflector fiber respectively as shown in Fig 3. Here,

$$L_0 = L_1 + L_2 + G, \quad G \ll L_0 \quad (3)$$

Because the air-gap is very small in comparison to the gage length, and because the CTE of the capillary tube is quite close to the CTE of the fibers, the sensor inherently has very small TCS at the atmospheric pressure. However the CTE of the capillary tubing is expected to increase under a higher pressure range where these sensors will be used. In other words, the TCS would become worse especially at the pressure range of interest. The higher the pressure, the worse the TCS would be.

To avoid the TCS aggravation due to the high pressure, the sensor design could be manipulated. The thermal expansion coefficient of the input fiber cannot be adjusted because the kind of fiber is determined, but any kind of fiber of the same cladding diameter can be used as the reflector fiber. Also the ratio between the lengths of the input and the reflector fibers can be adjusted to get a desired total effect.

It is expected that the CTE of a fiber is higher if the doping level is higher and the core size is larger. When this kind of fiber is used for the reflector fiber, the TCS, $\Delta G / \Delta T$, would be a higher negative value at the atmospheric pressure as reflected in the equation (2). When the higher pressure of down-hole increases the CTE of the capillary tube, the TCS shall be compensated to the smaller value that we want, which should be zero at a certain point within the pressure range. If the TCS at the atmospheric pressure is reasonably controllable, the zero TCS point within the pressure range can be selectable, depending on the pressure range of the interest of the customers.

3. Experimental setup

Based on the reasoning described in the previous section, a few sensors of different design have been built using different fibers and different ratios between the lengths of the input and the reflector fiber. Those sensors were packaged using a unique design which preserves the original pressure sensitivity and the original TCS. Fig 5 shows the sensor calibration and the TCS test setup. Fig. 6 is the schematic diagram of it. To freeze the source profile for a better accuracy of the measurement, the temperature of the hermetically sealed case of the LED is stabilized using a TEC and a temperature controller. The packaged sensor was pressurized stepwise using a deadweight tester from 0 psig to 6000 psig.

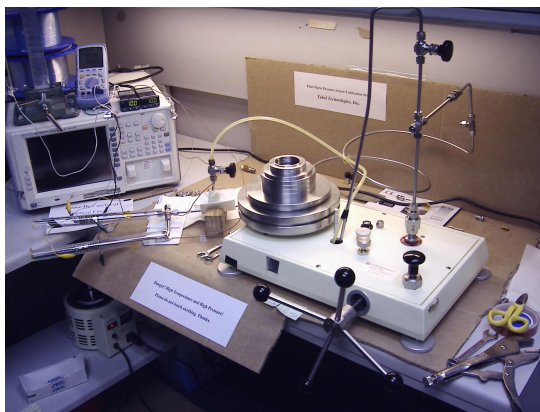


Fig.5. Calibration and temperature cross-sensitivity test setup

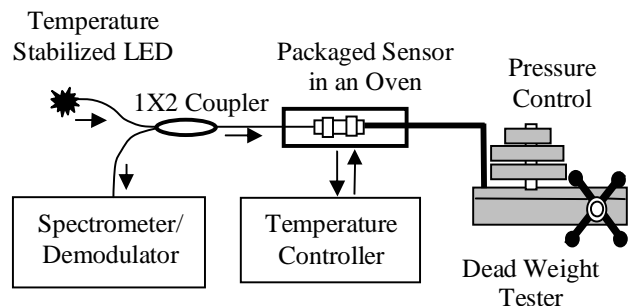


Fig. 6. Schematic diagram of the setup

Using a specially designed small oven and a temperature controller, the temperature of the packaged and pressurized sensors was controlled. The air-gap change is accurately and reliably monitored to determine the temperature cross sensitivities at various pressure levels using the surface system.

4. Experimental results

First of all, the TCS's at the atmospheric pressure for the differently designed sensors were evaluated to see if they are reasonably and practically controllable. Three different fibers were chosen for the reflector fiber. Fig. 7 shows the result. Using the fibers chosen for the reflector and by controlling the ratios between the lengths of the input fiber and the reflector fiber it was possible to get the TCS's at the atmospheric pressure as small as ~zero nm/°C (Fig 7-a) and as large as > -1.0 nm/°C (Fig 7-d). Pressure sensitivity for a gage length of 10 mm is calculated to be -0.71 nm/psi or -1.40 psi/nm using the equation of (1), which will be verified through pressure tests. Using the scale factor the -1.0 nm/°C TCS is translated into +1.4 psi/°C cross-sensitivity at the atmospheric pressure. Different sensors using the same fibers with the same ratios did not show the exactly same results but have some random distributions in TCS's at the atmospheric pressure. However they showed a strong tendency in smaller or larger TCS's depending on the design, which makes the free selection of the desired TCS value possible. Evaluating the TCS's of 100% sensors built at the atmospheric pressure is no problem in practice.

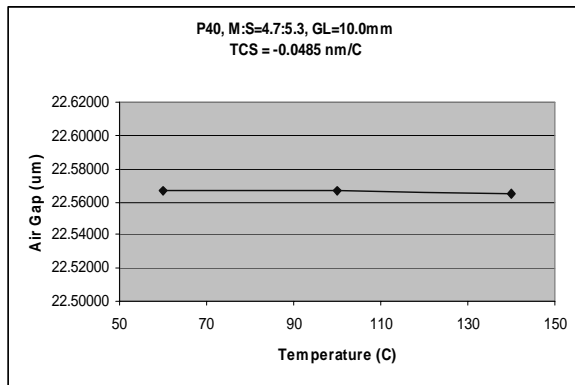


Fig. 7-a) TCS = - 0.0485 nm/°C

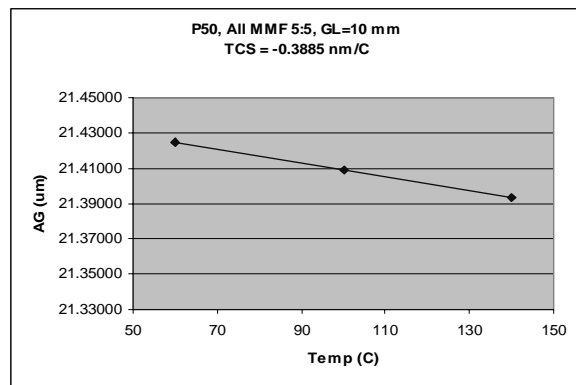


Fig. 7-b) TCS = - 0.3885 nm/°C

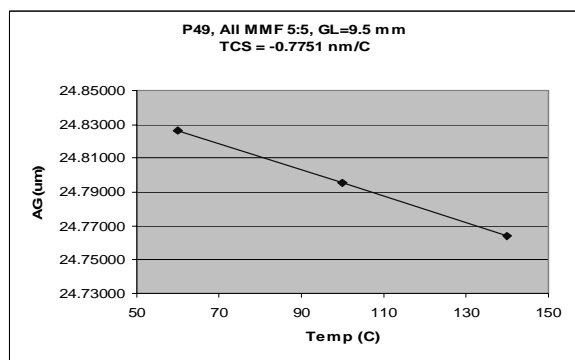


Fig. 7-c) TCS = - 0.7751 nm/°C

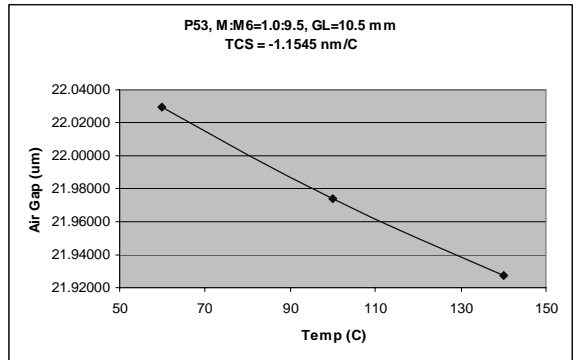


Fig. 7-d) TCS = -1.1545 nm/°C

Fig. 7. Different temperature cross-sensitivities at the atmospheric pressure for differently designed sensors

Some selected test sensors were packaged as shown in fig 4 for the pressure test. Fig 8 shows the pressure test result for a sensor which has the TCS of -0.3435 nm/°C at the atmospheric pressure. As shown in the Fig 8-a) through Fig. 8-d), as the pressure increases, due to the CTE change of the capillary tube, the TCS varies. Starting with the intentional

negative slope at the atmospheric pressure (Fig 8-a), as the pressure increases, the negative slope gets smaller (Fig. 8-b) and eventually changed to a positive slope (Fig. 8-c and d). Between 2200 psi and 4200 psi, must the zero TCS point exist.

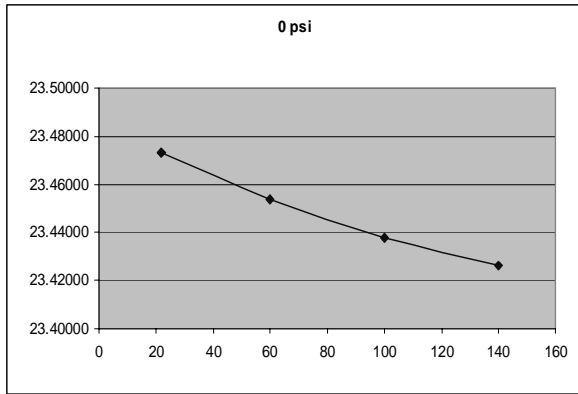


Fig. 8-a) At 0 psig, TCS = -0.3435 nm/°C

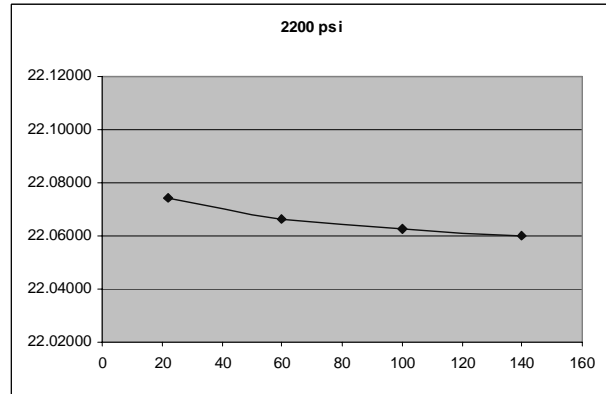


Fig. 8-b) At 2200 psig, TCS = -0.0765 nm/°C

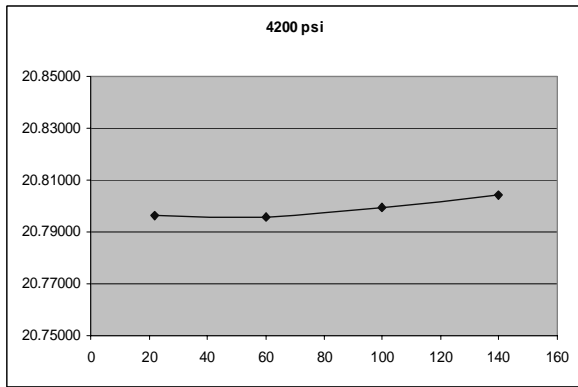


Fig. 8-c) at 4200 psig, TCS = +0.1058 nm/°C

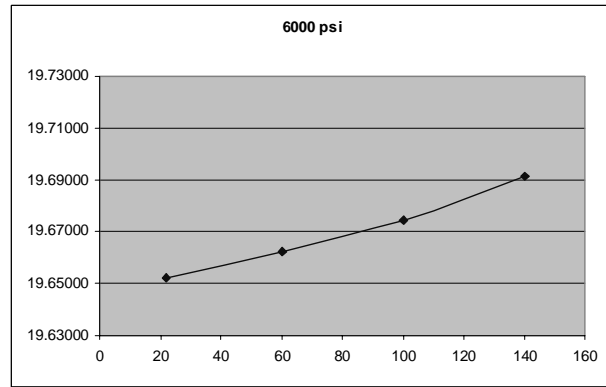


Fig. 8-d) at 6000 psig, TCS = + 0.3645 nm/°C

Fig. 8. Temperature cross-sensitivity change for the different pressure levels

Fig 9 shows the calibration curves for different temperatures for a couple of representative sensors. One is a sensor that has almost zero TCS at the atmospheric pressure (Fig. 9-a) and the other is the sensor of Fig 8 which has -0.34 nm/°C TCS at the atmospheric pressure. Both sensors show a very good linearity and repeatability. Both sensors use the same capillary tube with the same gage lengths. The slope changes, in other words the sensitivity or scale factor changes, due to the temperature change for the two sensors are quite close (0.00012050 nm/psi/°C for Fig 9-a and 0.00011762 nm/psi/°C for Fig 9-b for the temperature range of 100°C ~140°C). In the case of Fig 9-a, TCS is best at 0 psig, and worst at 6000 psig. In the case of Fig 9-b, with the sensor design change, the zero TCS point is shifted to around 3000 psig, and the TCS aggravation due to the increased pressure becomes about half of the case of Fig 9-a) at the maximum pressure point. Fig. 9-b) is just a replotting of the same data for Fig 8-a) through 8-d)

It is possible to make TCS at atmospheric pressure higher than -1.0 nm/°C using a different fiber for the reflector fiber, so the zero TCS point can be shifted to higher than 6000 psi. Whether the zero crossing point should be shifted to the maximum point or mid-point or in between those two within the pressure measurement range depends on the customer requirement considering the well temperature variation, temperature information availability, and the pressure range of interest. What is certain and important is that, for a limited pressure range of the choice, the temperature cross-sensitivity is almost zero.

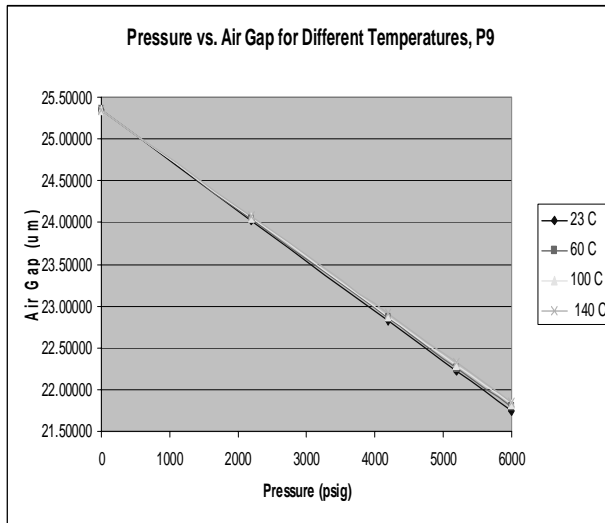


Fig. 9-a) for TCS ≈ 0 at the atmospheric pressure

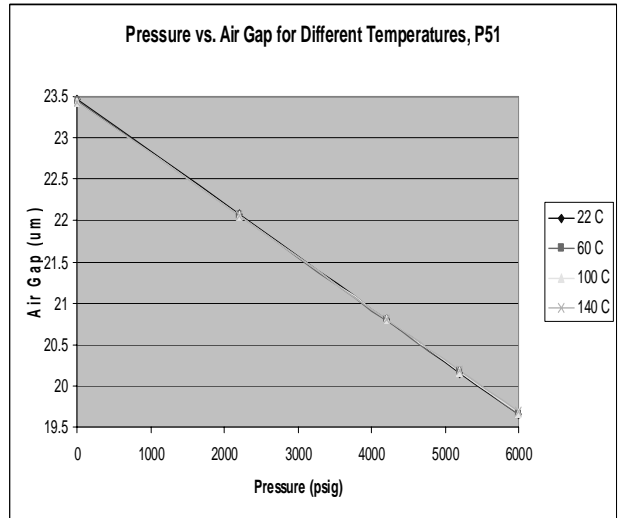


Fig. 9-b) zero TCS point shifted to ~ 3000 psi

Fig. 9. Calibration curves for different temperatures

5. Analysis of the results

As confirmed through the experiments, the coefficient of thermal expansion (CTE) of the capillary tube increases under the high pressure. This change slightly affects the slope (nm/psi) of the calibration curve for different temperatures as can be seen in the Fig. 9-a) and 9-b). The slope change is confirmed to be quite consistent and predictable. In the temperature range of $100^{\circ}\text{C} \sim 140^{\circ}\text{C}$ it was estimated to be:

$$(\Delta G/\Delta P)/\Delta T = +0.00012 \text{ (nm/psi)/}^{\circ}\text{C} \quad (4)$$

From this important number with the pressure scale factor (psi/nm), the following engineering formulae, (6) through (8), can be drawn. The scale factor was evaluated to be average of -0.625 nm/psi or -1.6 psi/nm in the case of 10mm gage length. This exhibits a slight discrepancy with the calculated value of -1.4 psi/nm . This is considered to be caused by the differences between the known and the actual values of the material mechanical properties (Young's modulus, Poisson's ratio) and/or of the dimensions of capillary tubing. Fig 10 shows the concept of the zero TCS point shift in relation with the formulae. Even though these are for a specific design of 10mm gage length with a specific capillary tube, these formulae could be easily adapted to the designs of different dimensions because the relations are very linear.

TCS change due to a pressure change ($\Delta\text{TCS}/\Delta P$):

$$+0.00012 \text{ (nm/}^{\circ}\text{C)/psi or -0.000192 (psi/}^{\circ}\text{C)/psi} \quad (5)$$

To have the zero TCS point at a pressure P_0 psi, the sensor should have a TCS of:

$$-0.00012 \times P_0 \text{ (nm/}^{\circ}\text{C) at the atmospheric pressure} \quad (6)$$

Using the (5), the TCS aggravation due to a deviation from the zero crossing point (P_0) would be:

$$-0.000192 \times (P - P_0) \text{ psi/}^{\circ}\text{C} \quad (7)$$

Assuming a mid-point zero TCS within a pressure measurement range, the worst TCS would be:

$$0.000192 \times (P_{\max} / 2) \text{ psi/}^{\circ}\text{C} \quad (8)$$

For an example of 6000 psi maximum pressure range with the zero crossing point at 3000 psi, worst TCS would be $-0.576 \text{ psi/}^{\circ}\text{C}$ at 6000 psi and $+0.576 \text{ psi/}^{\circ}\text{C}$ at 0 psi. If the measurement range of major interest is reduced to the range of 2000 ~ 4000 psi, the worst TCS would be reduced to $\pm 0.192 \text{ psi/}^{\circ}\text{C}$. The temperature cross-sensitivity is truly almost zero around the 3000 psi.

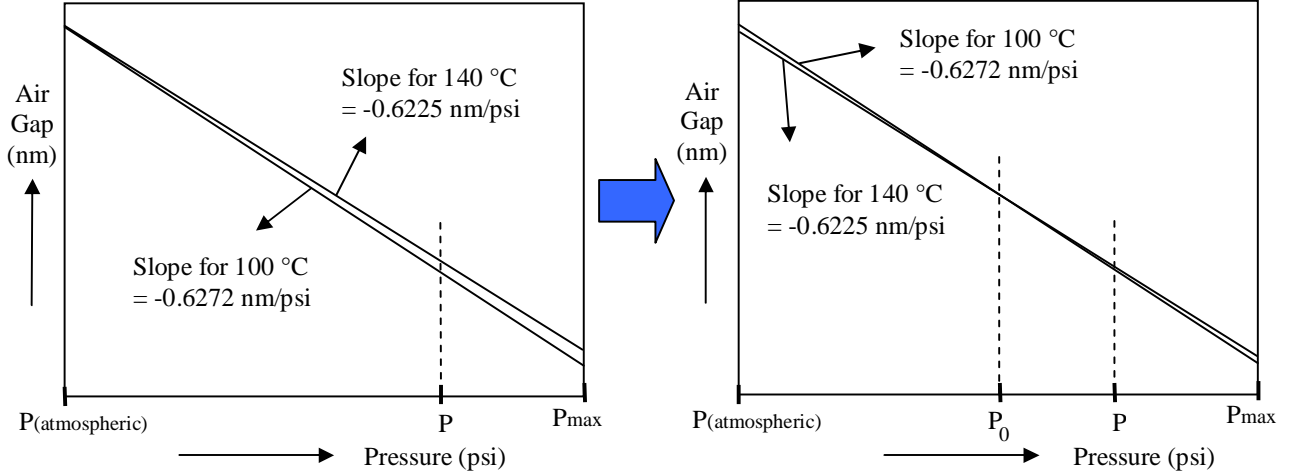


Fig. 10-a) TCS = 0 at the atmospheric pressure

Fig. 10-b) Zero crossing point shifted, TCS = 0 at P_0

Fig. 10. Concept for the zero TCS point shift and the TCS deviation from the zero crossing point

Finally, following is to evaluate the CTE increase factor with the pressure, percent increase per psi (%/psi), of the capillary tubing used:

From equation (2),

$$\text{at } P_0, 0 = \alpha_0 \cdot L_0 - (\alpha_1 \cdot L_1 + \alpha_2 \cdot L_2) \quad (9)$$

$$\text{at } P, TCS_P = \alpha_0' \cdot L_0 - (\alpha_1 \cdot L_1 + \alpha_2 \cdot L_2) \quad (10)$$

$$\text{by (10)-(9)} \quad TCS_P = (\alpha_0' - \alpha_0) \cdot L_0 \quad (11)$$

$$\alpha_0' = \alpha_0 + \frac{TCS_P}{L_0} = \alpha_0 + \Delta\alpha \quad (12)$$

$$\Delta\alpha = \frac{TCS_P}{L_0} \quad (13)$$

$$\text{Percent increase per psi (\%/psi)} = \frac{\frac{\Delta\alpha}{\alpha_0} \cdot 100\%}{P - P_0} \quad (14)$$

Using the equations (13), (14) and the experimental results (for $P - P_0 = +1000 \text{ psi}$, the $TCS_P = +0.12 \text{ nm/}^{\circ}\text{C}$), the percent increase of the CTE of the capillary tube is estimated to be $2.4 \times 10^{-5} \text{ \%/psi}$.

The engineering coefficient (5), $\Delta TCS/\Delta P$, is for the fused silica tubes and for the specific gage dimension. Due to the linear relations involved with this type of sensor design, the evaluation of the coefficient for different designs will be simple. This will be further confirmed through the extended sensor building and testing.

6. Conclusion

A practical, simple, and low-cost method to minimize the temperature cross-sensitivity (TCS, $\Delta P/\Delta T$) of the EFPI pressure sensor has been developed and the feasibility been proved through the careful experiments and analysis. Through the analysis of the experimental results, practical formulae that could be used for the sensor design were drawn. Once the sensor material and the dimensions for the EFPI are determined, the TCS deviation from the zero crossing point ($\Delta TCS/\Delta P$) is determined. With the specific design of 10 mm gage length of the silica capillary tube used for this experiment, the $\Delta TCS/\Delta P$ was evaluated to be -0.000192 (psi/°C)/psi. Using this coefficient, for an example, the TCS of a sensor which has zero TCS point at 6000 psi would have worst TCS of ± 0.192 psi/°C in the range of 5000 ~ 7000 psi. Using the low cost manipulation of the sensor design, the true 'zero' TCS point can be shifted to any point of interest within the pressure measurement range.

7. Acknowledgement

The commercialization of the EFPI pressure sensor by Tubel Technologies has been possible based on the previous work of Center for Photonics Technology (CPT) at Virginia Tech., VA. Authors would like to express great thanks to Professor Anbo Wang, Professor Gary Pickrell, and Dr. Juncheng Xu.

REFERENCES

1. Thomas G. Giallorenzi, Joseph A. Bucaro, Anthony Dandridge, et al., *Optical fiber sensor technology*, IEEE Journal of Quantum Electronics, Vol. QE-18, No.4, pp.626 -665, April 1982
2. John Dakin and Brian Culshaw, *Optical Fiber Sensors Volume 4, Application, Analysis, and Future Trends*, 1997, Published by Artech House Inc.
3. Andreas Othonos, Kyriacos Kalli, *Fiber Bragg Gratings – Fundamentals and Applications in Telecommunications and Sensing*, 1999, Published by Artech House Inc.
4. S. Tanaka, M. Satoh, and Y. Ohtsuka, *Fiber-optic interferometric hydro-pressure sensor immune from temperature disturbances*, Tenth international conference on optical fiber sensors, Proceedings of SPIE Vol. 2360, 1994
5. Wojtek J. Bock and Wacław Urbanczyk, Temperature desensitization of a fiber-optic pressure sensor by simultaneous measurement of pressure and temperature, *Applied Optics*, Vol. 37, No. 18, June 1998
6. Bing Qi, Gary Pickrell, Po Zhang, et al., *Fiber optic pressure and temperature sensors for oil down hole application*, Proc. SPIE Vol.4578
7. Anbo Wang, Hai Xiao J. Wang, et al., *Self-calibrated interferometric-intensity-based optical fiber sensors*, *Journal of Lightwave Technologies*, vol. 19, No. 10, October 2001